

An experimental and theoretical study of pyrolysis mechanism of *o*-, *m*- and *p*-benzenediols

Yuki Furutani,¹ Shinji Kudo,² Jun-ichiro Hayashi,² and Koyo Norinaga²

¹Interdisciplinary Graduate School of Engineering, Kyushu University

²Institute for Materials Chemistry and Engineering, Kyushu University
Kasuga-koen, Kasuga, Fukuoka 816-8580, Japan,

Abstract

To elucidate the pyrolysis mechanism of benzenediol isomers derived from biomass pyrolysis, pyrolysis-gas chromatography (Py-GC) experiments were performed to reveal the distribution of the pyrolytic products under different temperatures. Concurrently, quantum chemical calculations were conducted to analyze and verify the thermal decomposition and product formation pathways.

1. Introduction

The pyrolysis technique is implemented to convert biomass into valuable fuel gases which can be directly utilized or refined as a liquid fuel and chemical products. During the pyrolysis process, solid fuels are converted to volatiles and char in the primary pyrolysis, and the volatiles cracking occur to yield both light-gas and high molecular compounds like polycyclic aromatic hydrocarbons. Investigation of the vapor-phase reaction pathways of models representing the volatiles is helpful and significant to understand and simplify the reaction network. Phenolic compounds are well-documented byproducts from the thermal degradation of biomass, and in this study *ortho*-, *meta*- and *para*-benzenediol isomers (Fig. 1) are employed as models of the volatiles.

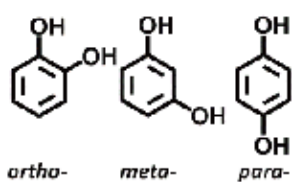


Fig. 1: Benzenediol isomers

The studies concerning the pyrolysis mechanism are, however, limited. The objective of this research is to analyze the pyrolysis mechanism of the benzenediols by combining experimental studies with theoretical methods.

2. Experiment

Pyrolysis mechanism of benzenediols was investigated by a two stage tubular reactor (TS-TR)¹ connected with GC. TS-TR was made of quartz and consists of two zones divided by a quartz wool filter. The sample was dropped into the

bottom of the first hot zone and vaporized at 650 – 950 °C with 0.3 s of residence time (t_r). Then, volatiles were flown into the secondary zone with helium carrier gas at 241 kPa with $t_r = 3.6$ s. Passing the secondary zone, volatiles were directed into GC column and further identified by GC detector.

Fig. 2 illustrates the yields of CO and CO₂. CO was a major final product with maximum yields of 25.1, 19.4, and 24.3 wt% formed from *o*-, *m*- and *p*-benzenediols, respectively. It was worthy to note that much more CO₂ (15.5 wt%) were generated from *m*- than from *o*- and *p*-benzenediols (1.0 and 0.8 wt%).

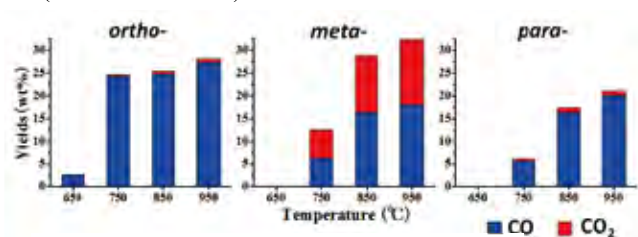


Fig. 2: Yields of CO and CO₂

3. Theoretical calculation

Fig. 3 shows the possible unimolecular thermal decomposition pathways for *m*-benzenediol, **R**, losing CO and CO₂. Equilibrium geometries and transition structures were optimized by use of a series of high accuracy methods including a complete basis set extrapolation, the CBS-QB3 composite method. The activation energies at each reaction step were obtained from the difference between the energies of the transition state and the reactants.

The decomposition commenced with fission of one of the O-H bond (step 1), and then forming *m*-semiquinone radical, **M1**. There are two decomposition pathways for **M1**. In the first channel, the aromatic ring contracted to form **M2**, followed by breaking a C-C bond of the three-membered ring and subsequently generating **M5** and CO molecular. The second channel affords the formation of *m*-benzoquinone biradical, **M6**, generated by the O-H bond dissociation (step 2). Ring-closing and cleavage of the six-membered ring in **M6** occur to form **M7** and **M8** followed by cyclization to form a five-membered ring intermediate state **M11**. After the formation of **M11**, the ketone radical group combines with carbon site on the carbonyl radical group to form **M12**. Then, **M13** is generated by breaking a C-C bond of the four-membered ring, and subsequently losing CO₂.

Fig. 4 shows temperature-dependency of activation energies for step 1 and step 2. This figure indicates that two activation energies showed little change, and over the entire temperature range the step 1 maintained the superiority over the step 2. For all reaction pathways toward CO and CO₂ elimination, therefore, the rate-determining step was commonly a step 1. Consequently, our theoretical calculation supported the experimentally-detected CO₂ expulsion from *m*-

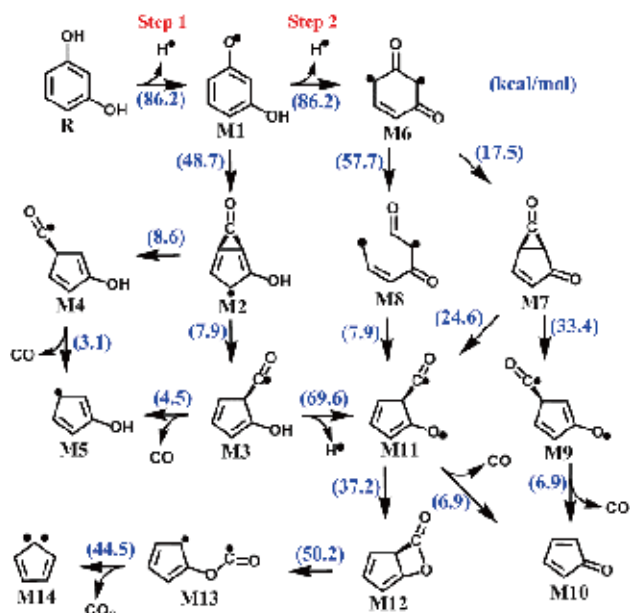


Fig. 3: Reaction pathways in the unimolecular decomposition of **R**. All values are activation energies at each reaction step.

benzenediol pyrolysis.

A five-membered ring **M14** is expected to capture a H atom in gas phase, followed by the formation of naphthalene,

C₁₀H₈, (Rxn-1)² or cyclopentadiene,

C₅H₆, (Rxn-2)³ Total reactions with the formation of CO₂ can be described as follows:

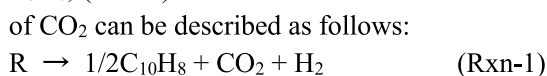


Fig. 5 shows the results of ΔG_0 of Rxn-1 and Rxn-2 at different temperatures (300 K to 1700 K at the interval of 50 K) at the CBS-QB3 level. Fig. 5 revealed that ΔG_0 of Rxn-1 and Rxn-2 remained negative values, which indicated that these reactions with the formation of CO₂ spontaneously could occur over the entire temperature range. Therefore, this result would be more evidence supporting the proposed reaction pathways leading to the CO₂ formation.

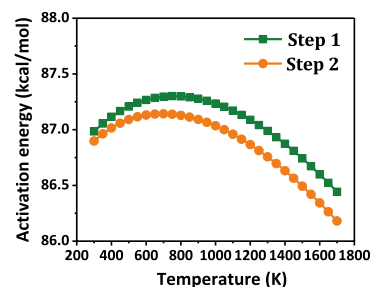


Fig. 4: Temperature-dependent activation energies

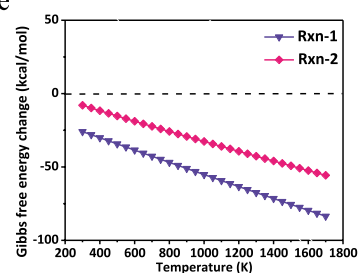


Fig. 5: Standard Gibbs free energy changes

4. Conclusion

The experiment revealed that although CO was a main inorganic gas produced from the pyrolysis of the three isomers, much more CO₂ were detected from *m*- than from *o*- and *p*-benzenediols. Our calculation results demonstrated that the rate-determining step in all reactions was the first-stage O-H bond dissociation reaction, and the reaction with the formation of CO₂ spontaneously could occur over the entire temperature range.

References:

1. Norinaga, K. et al.: *Biomass Bioenergy* **69**, 144 (2014).
2. Scheer, A. M. et al.: *J. Phys. Chem. A* **115**, 13381 (2011).
3. Melius, C. F. et al.: *Symp. Combust.* **26**, 685 (1996).